

Voltage-Dependent Gating in a “Voltage Sensor-Less” Ion Channel

Harley T. Kurata^{1*}, Markus Rapedius², Marc J. Kleinman^{3,4}, Thomas Baukrowitz², Colin G. Nichols^{3,4*}

1 Department of Anesthesiology, Pharmacology, and Therapeutics, University of British Columbia, Vancouver, Canada, **2** Institute of Physiology II, Friedrich Schiller University, Jena, Germany, **3** Department of Cell Biology and Physiology, Washington University School of Medicine, St. Louis, Missouri, United States of America, **4** Center for Investigation of Membrane Excitability Disorders (CIMED), Washington University School of Medicine, St. Louis, Missouri, United States of America

Abstract

The voltage sensitivity of voltage-gated cation channels is primarily attributed to conformational changes of a four transmembrane segment voltage-sensing domain, conserved across many levels of biological complexity. We have identified a remarkable point mutation that confers significant voltage dependence to Kir6.2, a ligand-gated channel that lacks any canonical voltage-sensing domain. Similar to voltage-dependent Kv channels, the Kir6.2[L157E] mutant exhibits time-dependent activation upon membrane depolarization, resulting in an outwardly rectifying current-voltage relationship. This voltage dependence is convergent with the intrinsic ligand-dependent gating mechanisms of Kir6.2, since increasing the membrane PIP₂ content saturates Po and eliminates voltage dependence, whereas voltage activation is more dramatic when channel Po is reduced by application of ATP or poly-lysine. These experiments thus demonstrate an inherent voltage dependence of gating in a “ligand-gated” K⁺ channel, and thereby provide a new view of voltage-dependent gating mechanisms in ion channels. Most interestingly, the voltage- and ligand-dependent gating of Kir6.2[L157E] is highly sensitive to intracellular [K⁺], indicating an interaction between ion permeation and gating. While these two key features of channel function are classically dealt with separately, the results provide a framework for understanding their interaction, which is likely to be a general, if latent, feature of the superfamily of cation channels.

Citation: Kurata HT, Rapedius M, Kleinman MJ, Baukrowitz T, Nichols CG (2010) Voltage-Dependent Gating in a “Voltage Sensor-Less” Ion Channel. *PLoS Biol* 8(2): e1000315. doi:10.1371/journal.pbio.1000315

Academic Editor: Richard W. Aldrich, University of Texas at Austin, United States of America

Received: August 7, 2009; **Accepted:** January 19, 2010; **Published:** February 23, 2010

Copyright: © 2010 Kurata et al. This is an open-access article distributed under the terms of the Creative Commons Attribution License, which permits unrestricted use, distribution, and reproduction in any medium, provided the original author and source are credited.

Funding: This work was supported by grants to CGN (National Institutes of Health (NIH) grant HL54171) and to HTK (NIH grant HL53268, a Canadian Institutes of Health Research (CHIR) Post-Doctoral Fellowship, and a CHIR operating grant). The funders had no role in study design, data collection and analysis, decision to publish, or preparation of the manuscript.

Competing Interests: The authors have declared that no competing interests exist.

Abbreviations: BK, large conductance potassium channel; CNG, cyclic nucleotide gated channel; KATP, ATP-sensitive potassium channel; Kint, internal potassium concentration; Kir, inwardly-rectifying potassium channel; Kv, voltage-gated potassium channel; MiRP, MinK-related peptide; PIP₂, phosphatidylinositol bis-phosphate; Po, open probability; SUR, sulfonylurea receptor; VSD, voltage-sensing domain.

* E-mail: hkurata@interchange.ubc.ca (HTK); cnichols@cellbiology.wustl.edu (CGN)

Introduction

While the entire complement of ion channels in a given cell contributes to the membrane voltage, only a subset (the voltage-gated cation channel family) responds significantly to changes in membrane voltage, and the molecular mechanisms underlying their voltage dependence remain the subject of considerable scrutiny [1–6]. Voltage-gated cation channels are typified by a modular 6-transmembrane segment (S1–S6) architecture, with the S5 and S6 helices forming a core pore-forming module, and the S1–S4 helices forming a canonical voltage-sensing domain (VSD) [7]. The VSD, and particularly a subset of positively charged amino acids in the S4 transmembrane segment, is essential for this voltage-dependent gating [8–10]. Inwardly rectifying potassium (Kir) channels possess a similar core K⁺-selective pore module but lack the VSD, and the gating mechanisms of this channel family are generally considered independent of voltage [11–13]. Instead, Kir channels are physiologically regulated by ligands specific to each channel subfamily, such as Gβγ subunits (Kir3 channels), protons (ROMK1 and others), or nucleotides (Kir6 channels) [14–16]. In addition, anionic “signaling” phospholipids such as PIP₂ interact with the cytoplasmic domains of all known Kir channels and increase channel activity [17].

Despite clear distinctions at the level of primary sequence, predictions of functional behavior based on structural properties do not always hold firm. For example, CNG channels contain a VSD but exhibit little intrinsic voltage-dependent gating [18]. A similar lack of voltage dependence is apparent in the voltage-sensor equipped KCNQ1 channel when assembled with certain accessory subunits (e.g., MiRP1 and 2) [19]. On the opposite end of this spectrum, KcsA channels, now an archetypal model for K⁺-selective pores, appear to exhibit some intrinsic voltage dependence despite lacking a canonical VSD [20,21]. A second important uncertainty arises in the mechanism of coupling between the voltage sensor and channel pore. In classical models of voltage-dependent gating (such as Shaker or other Kv channels), the VSD strongly influences opening/closing of the pore-forming domain, in the sense that channel open probability (Po) can be reduced to virtually 0 at sufficiently negative voltages and increased to near 1 upon depolarization [22]. In contrast, certain voltage-sensor equipped TRP channels exhibit sustained measurable open probability even at very negative voltages, together with much weaker apparent voltage dependence of gating relative to Kv channels [23–25], and incomplete closure can be engineered in classical Kv channels with open state stabilizing mutations at the S6 helix bundle crossing [26]. Such observations indicate that a

Author Summary

Ion channels are proteins that regulate the transfer of ions across the cell membrane. The ions travel via a pore formed by the different subunits that constitute the channels, and this pore can be gated by changes in the electrical field across cell membranes. The canonical mechanism underlying voltage dependence of gating relies upon a widely conserved structural motif called the voltage sensor, which undergoes conformational changes when charged amino acids within the motif respond to voltage and consequently affect the opening of the ion channel pore. In the present study, we have identified a non-canonical mechanism that surprisingly generates voltage-dependent changes in the activity of a ligand-gated ion channel that has no voltage sensor. Our observations suggest that ions flowing through the ion channel pore can significantly affect channel activity, and we suggest that voltage-dependent changes in ion distribution in the “cavity site” of the channel can influence opening and closing of the channel independent of canonical voltage sensors.

model of “tight coupling” between the VSD and pore does not apply to all channel types and that the pore domain itself may strongly influence open probability in some ion channels (whether equipped with a voltage sensor or not). In this regard, voltage-sensitive dynamics of the pore-forming module may not always be obvious in ion channels that are strongly governed by motions of the voltage sensor.

Through ongoing characterization of the Kir6.2 channel, we have begun to recognize that substitution of charged residues at pore-lining positions can affect channel gating in very unexpected ways. Kir6.2 is a two transmembrane domain inwardly rectifying K channel, clearly falling into the realm of “voltage sensor-less” ion channels, and assembles with sulfonylurea receptor subunits (SUR1, SUR2A, or SUR2B) to form K_{ATP} channels [27–29]. To date, most characterization of K_{ATP} gating has focused on its recognized physiological ligands (notably intracellular nucleotides and anionic phospholipids) [30–32]. The present study reveals remarkable voltage-dependent properties that arise in this “voltage-sensor-less” K_{ATP} channel, together with other unrecognized mechanisms of K_{ATP} channel regulation by intracellular ions. We have characterized a mutant Kir6.2 channel that exhibits marked voltage-dependent gating upon membrane depolarization. The voltage dependence of gating of Kir6.2[L157E] is convergent with ligand-dependent gating by ATP and PIP_2 and is likely to involve the same “gate” as these intrinsic physiological ligands of the K_{ATP} complex. We demonstrate that the voltage- and ligand-dependent gating of these channels is significantly affected by intracellular potassium ions, indicating an interaction between ion permeation and gating and providing a framework for understanding for what is likely to be a general feature of the superfamily of cation channels.

Results and Discussion

Voltage-Dependent Activation of the Kir6.2[L157E] Channel

We have characterized the properties of a number of Kir6.2 mutant channels substituted with various charged residues at pore-lining positions. Very unexpectedly, we observed that a single point mutation in the pore-forming subunit of K_{ATP} (Kir6.2[L157E]) generates channels that exhibit voltage-dependent activation (two different patches are depicted in Figure 1A).

At negative voltages, patches exhibit a steady-state non-deactivating current. Depolarizing voltage steps result in an instantaneous current jump followed by subsequent activation of current, resulting in an outwardly rectifying current–voltage relationship (Figure 1E). These observations contrast with behavior of WT Kir6.2 channels (Figure 1B), in which significant time-dependent activation is not typical and the macroscopic current–voltage relationship is nearly linear (Figure 1E). Residue 157 is located at a deep pore-lining position in the Kir6.2 inner cavity, directly adjacent to the putative “glycine hinge” (Figure 1C,D). While this single amino acid substitution introduces time-dependent activation somewhat similar to voltage-gated cation channels, the lack of a canonical VSD and a weaker voltage dependence relative to classical Kv channels implies a fundamentally different mechanism is at work (Figure 1D).

The effects of glutamate substitution at residue 157 are position specific. We have examined glutamate substitution at multiple other pore-lining positions in Kir6.2 [33] and found no evidence of similar behavior in 129E, 160E, or 164E channels (see Figure S1). Glutamate substitution at position 168 results in somewhat unusual effects on conduction, including intrinsic inward rectification (in the absence of intracellular blockers), but these do not resemble the unique voltage-dependent activation of Kir6.2[L157E].

Open Probability Is Voltage Dependent in Kir6.2[L157E]

Several observations confirm that voltage-dependent activation of Kir6.2[L157E] is due to channel gating, rather than an alternative mechanism such as relief of block, a voltage-dependent change in conductance, or activation of an alternative channel type in the patch. Firstly, we examined the effects of ligands known to alter channel Po in WT Kir6.2 and other Kir6.2 channels, namely PIP_2 (which is stimulatory and enhances open state stability/open probability) and poly-lysine (which is inhibitory and reduces open state stability). After inside-out patch excision, voltage-dependent currents were inhibited by internal ATP (Figure 2A,B) indicating that currents were indeed carried by K_{ATP} channels. We subsequently applied either PIP_2 or poly-lysine to the cytoplasmic face of the membrane and subjected patches to a series of voltage steps. A pattern emerged in which PIP_2 application resulted in accelerated kinetics of activation and a reduction in the activating fraction of macroscopic currents. This effect could be saturated with sufficient PIP_2 application, to the point where an activating component of current was no longer apparent (Figure 2C). Application of poly-lysine, which reduces open probability of Kir channels by shielding negatively charged headgroups of anionic phospholipids (e.g., PIP_2) [34], led to opposite effects: slower activation kinetics and an increased activating fraction of current (Figure 2C,D). To further verify that observed currents are indeed carried by Kir6.2, we exploited the fact that the L157E mutation confers strong spermine sensitivity. Application of spermine to excised membrane patches resulted in complete current inhibition at depolarized voltages (Figure S2), confirming that the observed voltage dependence is intrinsic to these channels and that development of leak does not contribute to current properties observed after subsequent treatment with activating agents such as PIP_2 .

Manipulation of open state stability over a wide range (using PIP_2 or poly-lysine) illustrates a relationship between open state stability and the properties of voltage-dependent gating, demonstrated in normalized current records (Figure 2E) and in data from multiple patches (Figure 2F,G). Using ATP sensitivity (fractional inhibition in 10 μ M ATP) as an index of open state stability [30,31], there is a clear relationship between open state stability and both the activation time constant and the fractional activating

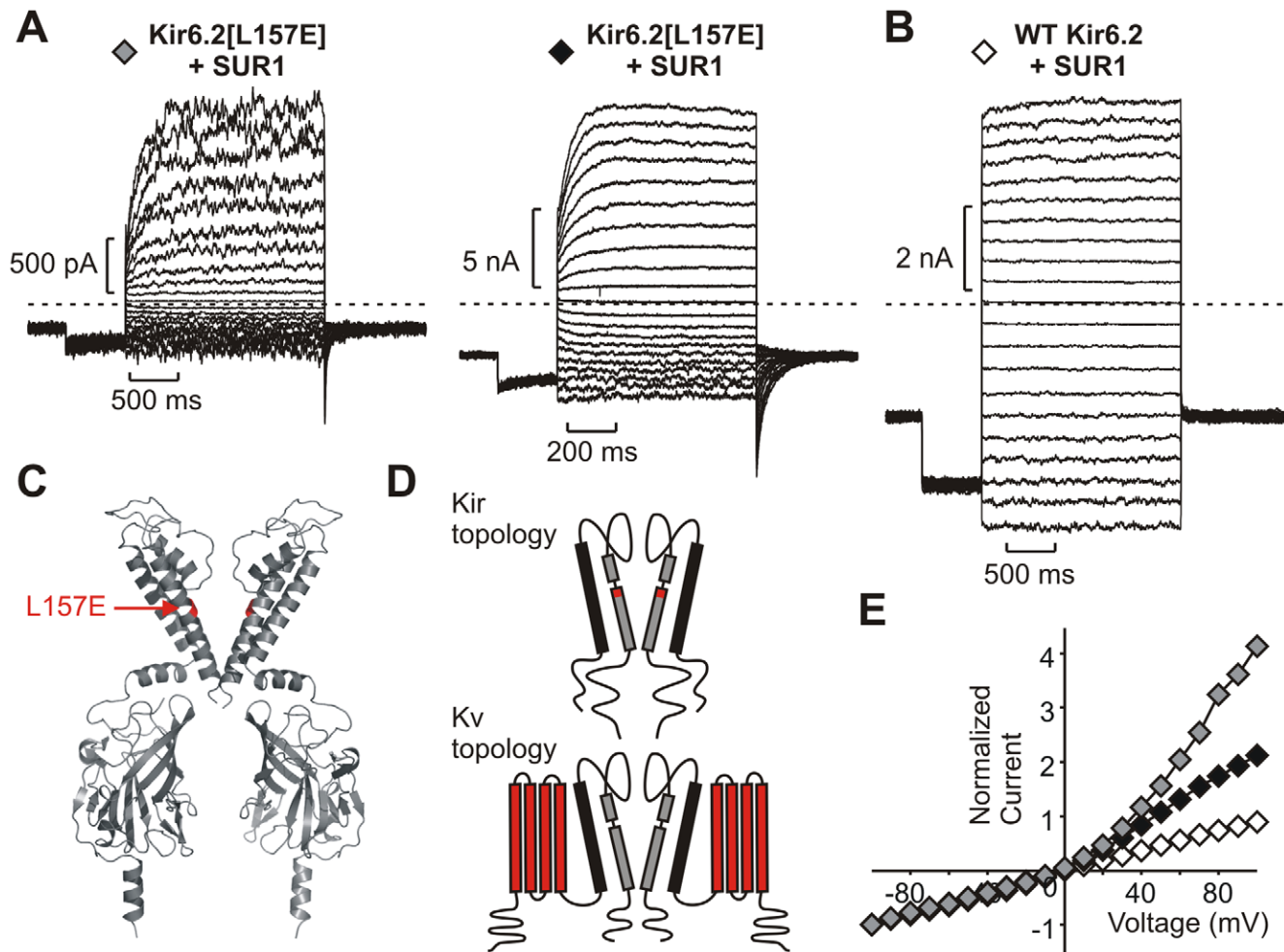


Figure 1. Voltage-dependent activation of Kir6.2[L157E] channels. (A,B) Representative inside-out patch clamp recordings from (A) two different Kir6.2[L157E] membrane patches and (B) a WT Kir6.2 membrane patch (both co-expressed with SUR1). Patches were pulsed to voltages between -100 and $+100$ mV, with a holding potential of -50 mV. (C) Molecular model of Kir6.2, with residue 157 highlighted in red. (D) Transmembrane topologies of Kir and Kv channel families, with elements underlying voltage-dependent gating colored red in each case. (E) Current-voltage relationships illustrating outward rectification of Kir6.2[L157E] channels. Symbols correspond to the recordings depicted in panels A–B. doi:10.1371/journal.pbio.1000315.g001

component of macroscopic current. At low open state stability (after poly-lysine, low P_o , channels very sensitive to ATP), the activating fraction is large and the activation kinetics are slow (Figure 2E, red trace, and Figure 2F,G). In contrast, at high open state stability (after PIP_2 , high P_o , channels weakly sensitive to ATP), the activating component of current decreases, and the activation time constant is accelerated (Figure 2F,G). PIP_2 exposures sufficient to saturate open probability virtually eliminate voltage-dependent gating (because channels are maximally open at all voltages, Figure 2E, green trace). The demonstrated relationship between channel P_o and voltage-dependent gating, and especially the loss of voltage dependence at saturating open probability, indicates that the gating of Kir6.2[L157E] arises primarily from voltage-dependent changes in P_o . Also, convergence of the novel voltage-dependent gating mechanism and intrinsic PIP_2 regulation suggests that voltage is influencing the ligand-operated (ATP/ PIP_2) gate of Kir6.2.

Multi-Tiered Kinetic Model of Voltage-Dependent Gating

It is notable that voltage-dependent properties can vary from patch to patch, as ambient lipid levels (likely PIP_2) vary (Figure 1A,B,

Figure 2A) [35]. The relationship between open state stability and voltage-dependent gating is further illustrated in Figure 3 and provides an additional perspective to the effects described in Figure 2. After excision, open probability was first brought to saturation by application of PIP_2 [30] (Figure 3A,i), and then iteratively reduced with brief poly-lysine applications (Figure 3A,ii–v). Currents after each poly-lysine exposure were normalized to the “fully activated” currents (condition (i)). Notably, at low open state stability (low PIP_2 levels, e.g., Figure 3A,v, or Figure 2D), currents at negative voltages are small but can increase several-fold upon depolarization. The result is a large activating fraction of outward current (in normalized traces, Figure 2E), although the absolute currents do not reach the same level as observed in higher PIP_2 conditions. As open state stability is increased, basal currents at negative voltages are larger, and the fraction of outward current that exhibits time-dependent activation is necessarily smaller. Importantly, the emergence of these patterns are not due to electrostatic effects on permeation, because neither PIP_2 or poly-lysine affect the Kir6.2 single channel conductance [31,34].

The steady-state voltage and PIP_2 dependence of activation of Kir6.2[L157E] can be reasonably well fit over a wide range of

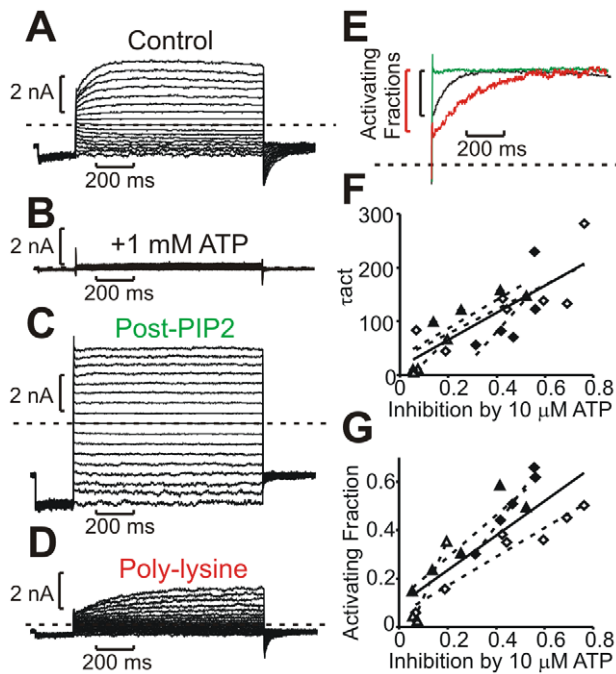


Figure 2. Voltage-dependent gating of Kir6.2[L157E] channels interacts with PIP₂-regulated open probability. (A–D) Representative current traces from a Kir6.2[L157E] membrane patch, (A) immediately after excision, (B) in 1 mM ATP, (C) after exposure to 5 μg/mL PIP₂, (D) after brief exposure to the PIP₂ antagonist poly-lysine. (E) Currents from A, C, and D are normalized to peak to illustrate the effects of basal open probability (determined by PIP₂) on activation kinetics and on the activating fraction of peak current. (F,G) Compiled data from 4 Kir6.2[L157E] membrane patches, illustrating the relationship between ATP sensitivity (an index of open state stability), and (F) activation kinetics or (G) activating fraction. At higher open state stability, a smaller fraction of the peak current exhibits time-dependent activation, and the kinetics of activation are markedly faster. In (F,G), data are presented from four patches, with each symbol type reflecting a different membrane patch. Dashed lines are linear regression fits to each individual patch, while the solid line is a fit to the entire data set. doi:10.1371/journal.pbio.1000315.g002

open state stability with a simple allosteric model (Figure 3B). The model describes an open-closed equilibrium (K_{CO}) governed by the membrane PIP₂ content, with channels able to occupy two different gating tiers distinguished by the K_{CO} equilibrium constant (the low Po tier has a small K_{CO} , and the high Po tier a higher K_{CO} —indicated by K_{CO}^* in Figure 3B). For clarity, the $K_{CO} \cdot [PIP_2]$ term directly reflects what we have referred to as “open state stability” thus far. The partition between high and low Po tiers is described by a voltage-dependent equilibrium constant (K_v). The model was fit simultaneously to data over a wide range of open state stability (by varying $[PIP_2]$ in the model). Similar experiments and analysis in four patches indicates a $K_v(0 \text{ mV})$ equilibrium constant of 0.7 ± 0.2 (with an effective valence of 0.7 ± 0.1) and a ~ 7 -fold stabilization of the K_{CO} equilibrium constant in the high Po tier ($K_{CO}^*/K_{CO} = 7.5 \pm 0.9$, this is also the value of the reversibility factor g).

Although a potential physical mechanism underlying voltage-dependent activation will be discussed in detail in subsequent sections, two elements of this kinetic model are worth noting. In simple terms, the model implies that the Kir6.2[L157E] channel operates in two gating tiers (high Po and low Po), with the partition between gating tiers influenced by voltage. Secondly, experimental data seem to preclude any simple model in which an open-closed

equilibrium is directly controlled by voltage—such models predict that sufficiently high voltages would open channels to a similar level (and sufficiently negative voltages would close channels), irrespective of basal open probability, a prediction that fails to match the observed behavior (Figure 3).

Single Channel Properties of WT and Kir6.2[L157E] Channels

We also measured currents from patches expressing small numbers of channels (1–5 per patch) to determine the effects of voltage on unitary conductance and P_o (Figure 4A). WT Kir6.2 and L157E channels exhibit similar single channel current magnitude, indicating that the L157E mutation has little effect on ion permeation (Figure 4B). Consistent with previous reports [36,37], single channel current-voltage relationships also exhibited mild inward rectification. Notably, L157E (but not WT) channels exhibit obvious increases in open probability at depolarized voltages (Figure 4A,C). Basal open probability tended to be fairly low in both WT and 157E patches, and so significant increases in open probability were frequently observed for L157E (Figure 4C, accounting for the large “activating fraction” observed in macropatch records—Figure 2E, Figure 3A,v).

Investigating the Voltage-Sensing Mechanism in Kir6.2[L157E]

(i) Internal cations affect gating of Kir6.2 channels. In addition to conferring voltage-dependent activation, mutations of Kir6.2 residue 157 surprisingly alter the effects of intracellular K^+ (K_{int}) on channel activity. In both WT Kir6.2 (Figure 5A) and Kir6.2[L157E] (Figure 5B), macroscopic currents (at -100 mV) are reduced in high K_{int} (300 mM), and increased in low K_{int} , effects that are substantially enhanced in L157E channels. To account for changes in reversal potential in different K_{int} , we used voltage-step protocols (e.g., Figure 5E–G) to calculate the change in macroscopic conductance (chord conductance), by measuring the change in current magnitude between -80 and -100 mV . This demonstrated that conductance of WT patches increased $\sim 40\%$, while L157E patches changed 4.5-fold with a switch from 300 mM K_{int} to 50 mM K_{int} (Figure 5D). Normalization to single channel current produced a similar result. This indicates that K^+ ions significantly influence the gating mechanism in Kir6.2[L157E] channels, with lower K_{int} favoring a higher open probability. Single channel records illustrate dramatic changes in P_o as K_{int} is altered (see Figure S3). Together, these observations indicate that intracellular K^+ ions significantly affect channel open probability in Kir6.2[L157E], and to a lesser degree in WT Kir6.2 channels.

Remarkably, the sensitivity to K_{int} can be reversed by introducing a positive charge at position 157. In Kir6.2[L157K] channels, increasing K_{int} causes an immediate and fully reversible increase of inward currents. This is opposite of what could be accounted for by changes in electrochemical driving force and contrasts dramatically with the effects of K_{int} in WT Kir6.2 and Kir6.2[L157E] channels. It is also notable that these effects are not selective for K^+ . In WT Kir6.2, L157E, and L157K channels, the effects of 300 mM K_{int} are closely mimicked by 50 mM K_{int} supplemented with 250 mM Na_{int} (Figure 5A–D).

Intracellular K^+ ions also dramatically influence gating kinetics of Kir6.2[L157E] (Figure 5E–H). In 300 mM K_{int} , activation kinetics are very slow, and the activating fraction of macroscopic currents is large, resembling the features observed for low Po patches (i.e., following poly-lysine application, Figure 2E). Conversely, currents in 50 mM K_{int} exhibit no time-dependent activation of currents, similar to the behavior of high Po patches

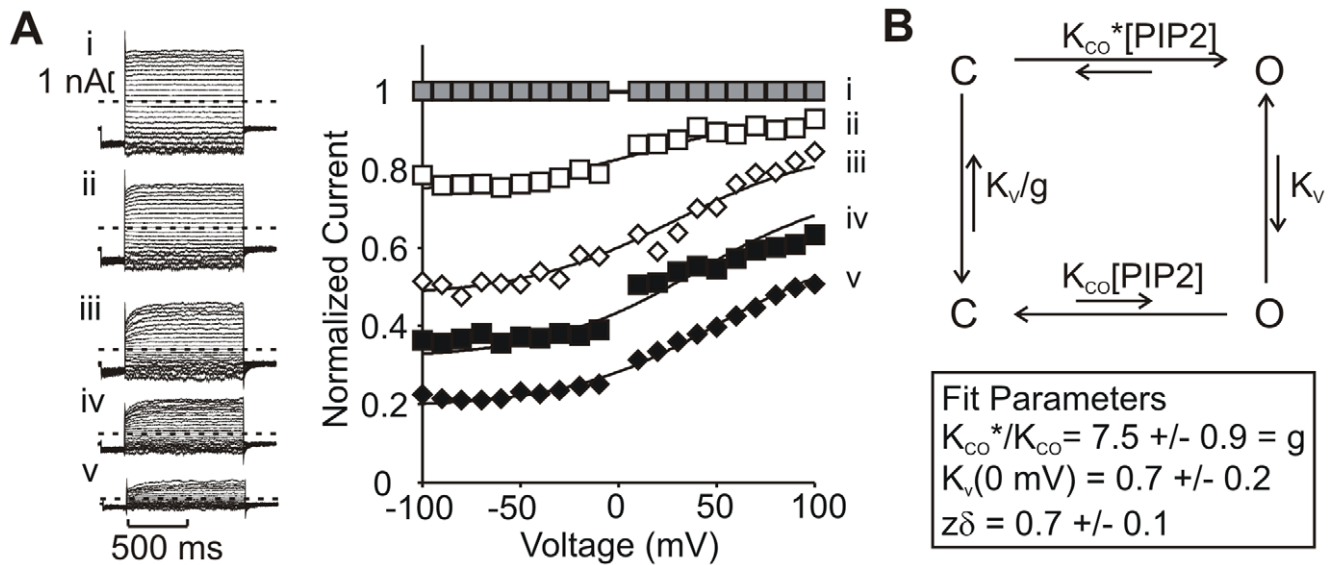


Figure 3. Kinetic model describing voltage-dependent activation of Kir6.2[L157E] over a range of voltage and basal open probability. (A) Current records collected after saturating open probability with PIP₂ (i), followed by progressive reduction of open state stability with brief applications of poly-lysine (ii–v). In the right-hand panel, steady-state currents were normalized to fully activated currents (record i) to illustrate the extent of activation at each voltage. (B) Kinetic model depicting two tiers of gating—a low Po tier (lower) and a high Po tier (upper). In the high Po tier, the KCO equilibrium constant is 7-fold larger. Equilibria between the high and low Po tiers are governed by the K_v constant, and g is a factor included to preserve reversibility ($g = K_{CO}^*/K_{CO}$). doi:10.1371/journal.pbio.1000315.g003

(i.e., after saturating PIP₂ treatment). Overall, these data indicate an especially strong interaction between permeant ions and gating of Kir6.2[L157E] channels.

(ii) Voltage-dependent occupancy of the cavity site in K⁺ channels. These observations suggest a “unifying” explanation for the unique behavior of Kir6.2[L157E] channels. Rather than acting as a sensor for changes in transmembrane voltage, we suggest that the L157E mutation generates an environment in which open state stability depends especially strongly on ion occupancy of the inner cavity (Figure 6). Intuitively, this is a straightforward idea: in the absence of a cation in the cavity ion binding site, repulsion between negatively charged side chains would drive the M2 helices apart, favoring channel opening at the helix bundle crossing [38,39]. Occupancy of the cavity ion site would mitigate this repulsion—157E carboxylates could approach more closely to the central axis of the pore, stabilizing channel closure relative to the unoccupied state. Consistent with our findings, these effects should be reversed with introduction of a positively charged sidechain at position 157 (e.g., L157K, Figure 5C,D). In general terms, the position specificity of the 157E effects (Figure S1) also seems well explained by this idea, because position 157 directly faces the cavity ion binding site and is adjacent to the putative “gating hinge” at glycine G156. Thus, even small motions in this region, perhaps driven by coulombic interactions between neighboring side chains and occupant ions, could be translated into significantly larger motions at the helix bundle crossing.

Such a mechanism may also account for the voltage-dependent activation of Kir6.2[L157E]. Specifically, kinetic models of ion permeation can predict substantial voltage-dependent changes in occupancy of selectivity filter sites and the cavity ion binding site. We have simulated voltage-dependent occupancy of the cavity ion binding site, based on published parameters for a model describing K⁺ permeation in KcsA. (Figure 6B,C) [40]. At *positive* voltages (or low K_{int}), the model predicts that occupancy of the cavity ion

binding site is low, because the voltage dependence of entry of the cavity ion into the selectivity filter is larger than the voltage dependence for “refilling” this site with an ion from the intracellular solution (Figure 6C). In this way, the gating effects (high Po) observed in low K_{int} can also be achieved at depolarized voltages. At *negative* voltages (or higher K_{int}), inward currents saturate the cavity ion binding site. Voltage-dependent cavity site occupancy can be predicted by permeation models in which the movement of the cavity ion into the selectivity filter is more voltage dependent than “refilling” of the cavity site with an intracellular ion and is consistent with the marked asymmetries in the characteristics of single channel openings carrying inward versus outward currents (see Figure S3). Given the generally accepted view that the membrane field is dissipated primarily across the selectivity filter [41,42], this seems a reasonable assumption. Also, the weak voltage dependence of cavity site occupancy over the experimental voltage range is comparable to the voltage dependence of channel activity (Figure 4).

Predictions of Permeation-Coupled Gating

An important concept of this model is that voltage does not directly drive the channel to open. Rather, channels open stochastically, and rearrangement of ion occupancy after channel opening governs the partition between high and low Po gating modes/tiers. Thus, if anything, the permeant ions themselves can be considered the “voltage sensors.” If this represents the predominant sequence of events during voltage-dependent activation, then the observed gating kinetics should depend primarily on intrinsic channel opening and closing rates (rather than the voltage-driven rate), and ATP stabilization of the closed state (prolongation of single channel interburst intervals) should affect the kinetics of channel opening. This behavior is indeed observed, and the effects can be quite dramatic (Figure 7A–E). Activation kinetics are slowed significantly in 10 μM ATP (Figure 7B,D). In some patches with sufficient current expression

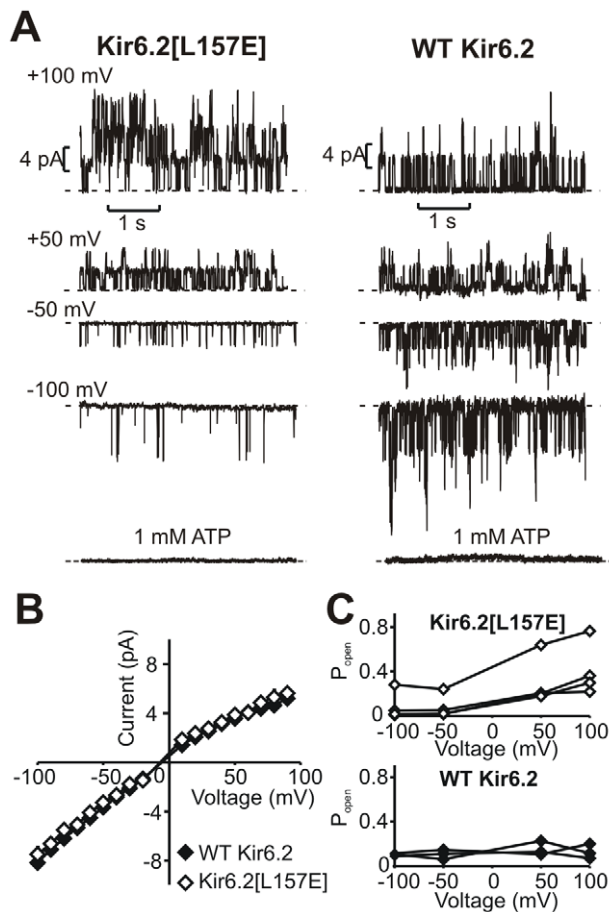


Figure 4. Depolarization increases open probability of Kir6.2[L157E] channels. (A) Current records from membrane patches containing few channels (likely three per patch) for Kir6.2[L157E] or WT Kir6.2 recorded in symmetrical 150 mM K^+ conditions. (B) Single-channel currents between -100 and $+100$ mV in WT Kir6.2 and Kir6.2[L157E] channels. The L157E mutation has no significant effect on single channel conductance. (C) Open probability of Kir6.2[L157E] (top) or WT Kir6.2 (bottom) channels measured from membrane patches containing 1–5 channels, between -100 and $+100$ mV ($n=3$ for WT and 4 for L157E). doi:10.1371/journal.pbio.1000315.g004

and appropriate open state stability, extremely slow activation was also observed in 100 μ M ATP (Figure 7C,D). This reflects the infrequency of opening in 100 μ M ATP—since openings occur rarely, channels will enter the high P_o tier very slowly. These effects can be rationalized by an extension of the simple allosteric model presented earlier (Figure 7E), with the addition of ATP-bound closed states reflecting stabilization of channel closure by ATP. This scheme is not intended to provide a complete description of ATP binding to K_{ATP} channels (see [43–45]). However, the model describes the important counter-regulation of K_{ATP} channels by ATP and PIP_2 [30,31] and predicts longer channel closures in the presence of ATP. In addition, channel opening upon depolarization and closure after hyperpolarization exhibit very weak voltage dependence ($z_{act} = 0.11 \pm 0.01$, $z_{deact} < 0.01$, Figure 7F,G). Again, this likely reflects the idea that the activation/deactivation kinetics are limited by the intrinsic bursting kinetics of the channel and that voltage is not driving the conformational changes that mediate gating.

Other Possible Effects of Internal Cations

We have also considered whether intracellular ions might affect channel activity by other mechanisms. We speculated that intracellular ionic strength might affect channel interactions with PIP_2 , and this appears to be a definite possibility. To examine PIP_2 interactions, WT Kir6.2 channel open probability was “rundown” with a high concentration of Mg^{2+} , and then exposed to various concentrations of diC8- PIP_2 , in both high and low ionic strength conditions (Figure 8). It is clear that in low ionic strength, channels are activated more completely and at lower diC8- PIP_2 concentrations. It appears that ionic strength can indeed alter channel- PIP_2 interactions, although it should be recognized that this experiment does not establish whether this is a direct effect of ionic strength, or an allosteric effect arising from the actions of ions within the pore (i.e., PIP_2 interacts with higher affinity with open channels, and so pore-mediated effects of ions on open probability could indirectly affect channel- PIP_2 interaction). Importantly, it seems unlikely that channel- PIP_2 interactions would be altered by mutations deep in the inner cavity—and thus the distinct properties of 157K versus 157E cannot be accounted for by this phenomenon. Nevertheless, there is a possibility that intracellular ionic strength affects K_{ATP} channel activity by multiple mechanisms.

Integrated Voltage- and Ligand-Gating

The K_{ATP} complex is a ligand-gated ion channel, in which diverse cytoplasmic ligands (most notably ATP, ADP, and PIP_2) determine open probability [30–32,46]. Nucleotide gating is a unique feature of the Kir6 subfamily, but PIP_2 dependence is common to all members [47]. In the present study, we have uncovered an additional dependence on intracellular cations that confers substantial voltage dependence. Changes in membrane voltage markedly alter the open probability of Kir6.2[L157E] channels, as confirmed by single channel and macroscopic current recordings. Saturation of P_o by PIP_2 (Figures 2, 3) abolishes voltage-dependent activation, confirming that activation reflects increased channel P_o . Strong voltage-dependent gating in the absence of a canonical VSD was unpredicted and is remarkable in at least two respects. Firstly, it demonstrates a mechanism by which permeating ions can influence the gating state of the pore-forming module. Secondly, it is imposed on the intrinsic ligand-dependent gating: the kinetic properties and extent of voltage-dependent activation clearly depend on PIP_2 (Figures 2, 3) and ATP levels (Figure 7), indicating that voltage is influencing the stability of the native PIP_2 /ATP-operated gate.

Converging lines of functional and crystallographic evidence suggest that ligand gating of Kir channels results from closure at or near the inner helix bundle crossing, as it does in Kv channels (see Text S1 for a detailed discussion of this point) [1,38,41,48–51]. Our data set is consistent with this model—permeant ions play an important role, but there is no ionic selectivity to the effect, and the critical residue (157) is located in the M2 helix, rather than in the selectivity filter. The voltage-dependent activation of Kir6.2[L157E] likely arises from a state preference for one orientation of permeating ions over another (specifically, whether the cavity site is occupied is vacant). Voltage-dependent ion occupancy, as modeled here (Figure 6), has been inferred from studies of voltage-dependent relief of TEA block in KcsA channels, in which TEA and K^+ interactions have been hypothesized to depend on voltage-dependent changes in ion occupancy profiles [40,52]. Although specific interactions with channel gating remain unexamined in KcsA and other channels, it is noteworthy that general features for this mechanism (the K^+ channel pore module, with a cavity ion binding site) are likely present in all K^+ channels,

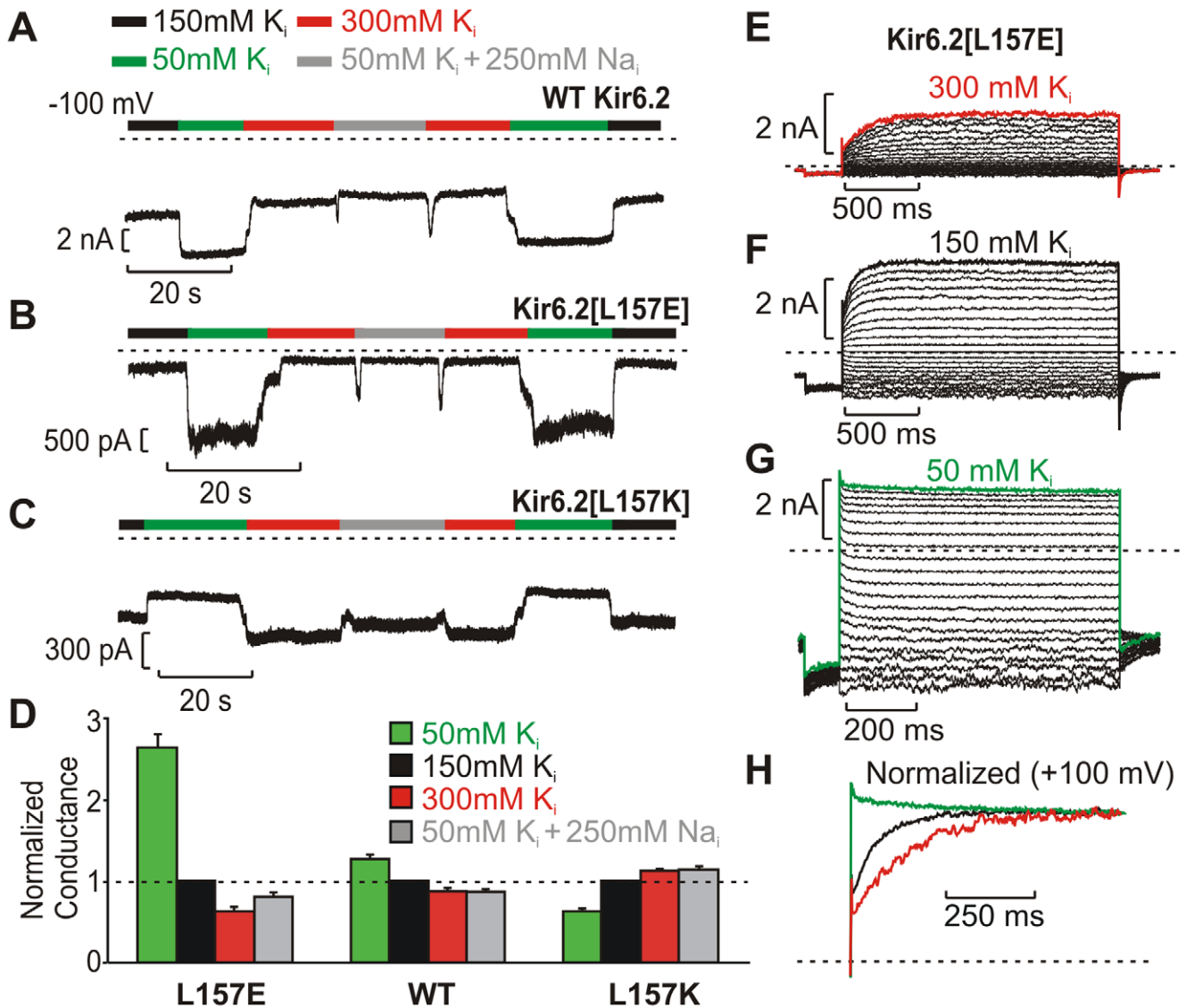


Figure 5. Position 157 affects the internal K⁺ sensitivity of Kir6.2. (A–C) Continuous current records at –100 mV depicting responses to altered internal ionic conditions in inside-out membrane patches expressing (A) WT Kir6.2, (B) Kir6.2[L157E], or (C) Kir6.2[L157K]. The L157E mutation exaggerates the response observed in WT Kir6.2, while the L157K mutation reverses the WT response to intracellular K⁺. (D) Using voltage-step protocols, the chord conductance between –100 and –80 mV was calculated in all K_{int} conditions and normalized to the conductance in 150 mM K⁺ in each patch ($n=29$ for WT Kir6.2, 19 for Kir6.2[L157E], and 20 for Kir6.2[L157K]). (E–G) Current records from a Kir6.2[L157E] inside-out patch, at voltages from –100 to +100 mV. (H) Currents elicited by a step to +100 mV, normalized to peak current, in the ionic conditions depicted in panels E–G. doi:10.1371/journal.pbio.1000315.g005

and the general principles could extend to other channel types irrespective of structure/sequence.

In Kv channels, Po is strongly controlled by the canonical VSD [22]. However, various channel types exhibit considerable diversity in the apparent strength of coupling between the voltage sensor and pore. As alluded to in the introduction, there is growing recognition of nominally “voltage-gated” channels that show far weaker voltage dependence than close *Shaker* homologues and exhibit persistent open probability at negative voltages [25]. Such features may indicate that coupling between the voltage sensor and pore is relatively weak and that the pore-forming module can significantly affect open state stability/open probability—indeed mutations in the helix bundle crossing region can result in persistent opening of Kv channels [26]. Furthermore, many voltage-gated channel assemblies, perhaps most notably the

KCNQ1/KCNE1 complexes, exhibit activation kinetics that appear to be considerably slower than the kinetics of voltage-sensor equilibration [53]. Similarly, a small voltage dependence is generally attributed to the final concerted opening step of the pore module in widely studied channels like *Shaker* and BK [22,54], although the mechanism for this voltage dependence is not well understood. Growing recognition of diverse non-canonical mechanisms of voltage sensing, in KcsA [20,21], in the present study, and in a recent report of introduced voltage dependence in CNG channels [55], suggest important avenues to investigate the role of the pore-forming module in controlling open probability.

Finally, while Kir6.2[L157E] exhibits an obvious voltage-dependent phenotype, the presence of a negatively charged side chain may not be an absolute requirement, since the same underlying feature is weakly detectable in WT channels. A small hint of this phenomenon

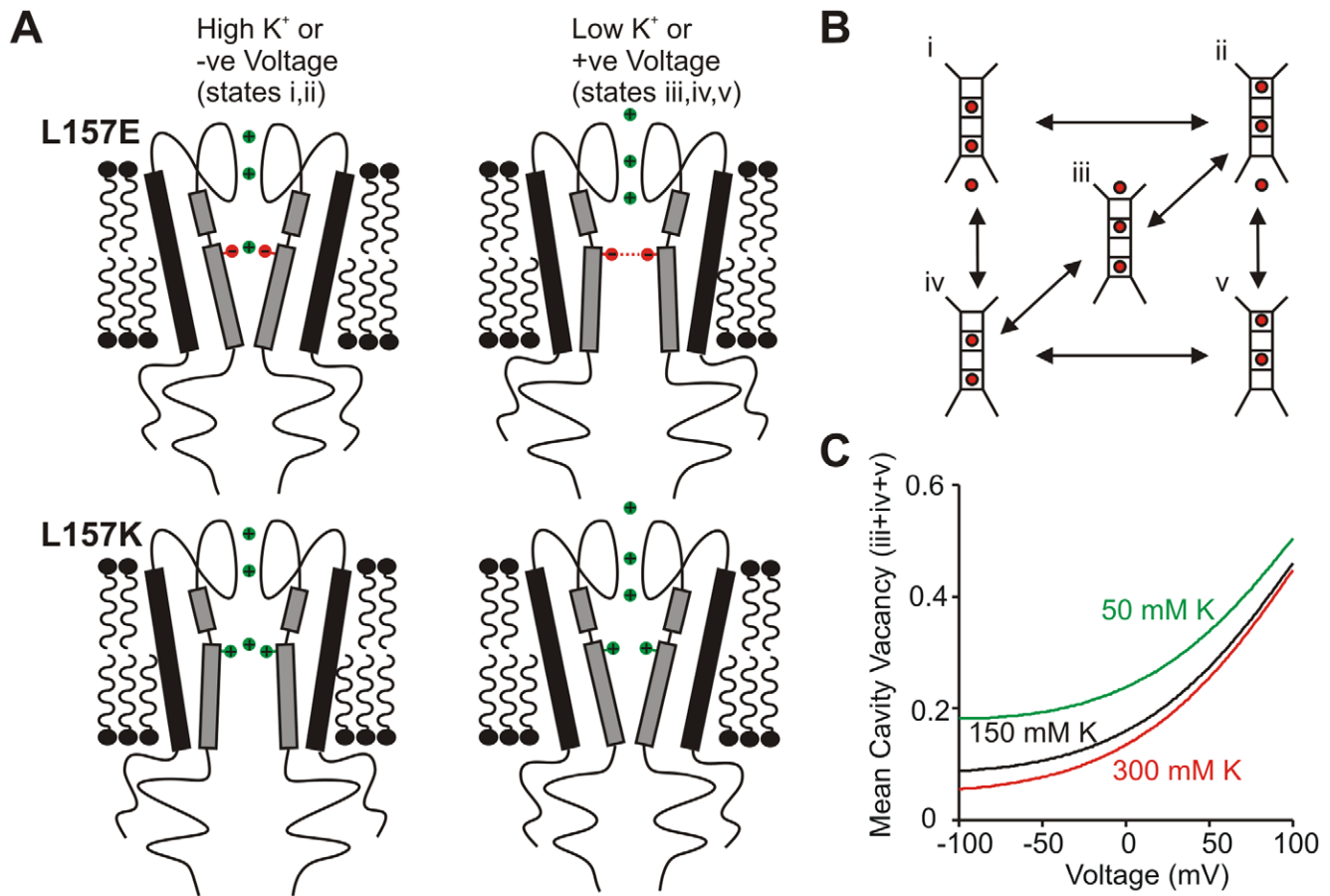


Figure 6. Hypothetical mechanism of convergent regulation by voltage and internal ions. (A) Cation occupancy in the cavity ion binding site will mitigate repulsion between glutamates substituted at position 157, favoring the closed state relative to conditions in which the cavity site is unoccupied. Introduction of a positive charge at position 157 would exhibit an opposite response to cavity site occupancy. (B) Permeation model, with boxes representing selectivity filter binding sites, flanked by an external binding site (top) and the cavity site (bottom). (C) Simulation of voltage and internal K^+ -dependent changes in mean occupancy of the cavity ion binding site (sum of probability of occupancy in states i+ii), using parameters generated to describe permeation through KcsA channels [40]. doi:10.1371/journal.pbio.1000315.g006

is apparent in Figure 1C, and we have included a more marked example in Figure S4. While not as dramatic as the voltage-dependent activation of Kir6.2[L157E], these features can be quite obvious and are exaggerated in modest inhibitory concentrations of ATP. These observations suggest that other features (beyond electrostatic interactions of charged side chains and the cavity ion) can generate some state preference for specific configurations of permeant ions. One potential candidate in K^+ channels is stabilization of the cavity ion by the pore helices, which may be more prominent in the closed versus open state [56], and thus might underlie some energetic preference for one configuration of permeant ions over another in different channel states.

Conclusions

We have characterized a unique and unexpected voltage-dependent activation feature of a ligand-gated Kir channel. The voltage dependence arises from voltage-dependent interactions of permeating ions with the same gate as that controlled by gating ligands, providing a unifying interaction between two fundamental processes of gating. The effects of the pore-forming module in regulating the kinetics and properties of voltage-dependent gating tend to be overlooked, since voltage dependence of cation channels is generally attributed to motions of a canonical VSD.

However, particularly in cation channels that exhibit relatively weak voltage dependence and persistent conductance at negative voltages, we suggest that the pore-forming module itself may be an important structural element in the regulation of voltage dependence and kinetics of channel gating.

Materials and Methods

Expression of K_{ATP} Channels in COSm6 Cells

Point mutations were prepared using the Stratagene Quick-change kit, on a background of WT mouse Kir6.2. COSm6 cells were transfected with pCMV6b-Kir6.2 (with mutations as described), pECE-SUR1, and pGFP using the Fugene 6 transfection reagent. Patch-clamp experiments were made at room temperature, using a chamber that allowed rapid solution exchange, or the Dynaflo capillary chip-based platform (Cellec-tricon Inc.), with DF-16 Pro II chips [57].

Data were typically filtered at 1 kHz, and signals were digitized at 5 kHz and stored directly on computer hard drive using Clampex software (Axon Inc.). The standard pipette (extracellular) and bath (cytoplasmic) solution used in these experiments had the following composition: 140 mM KCl, 1 mM K-EGTA, 1 mM K-EDTA, 4 mM K_2HPO_4 , pH 7.3. For 50 mM K_{int} , 300 mM K_{int} ,

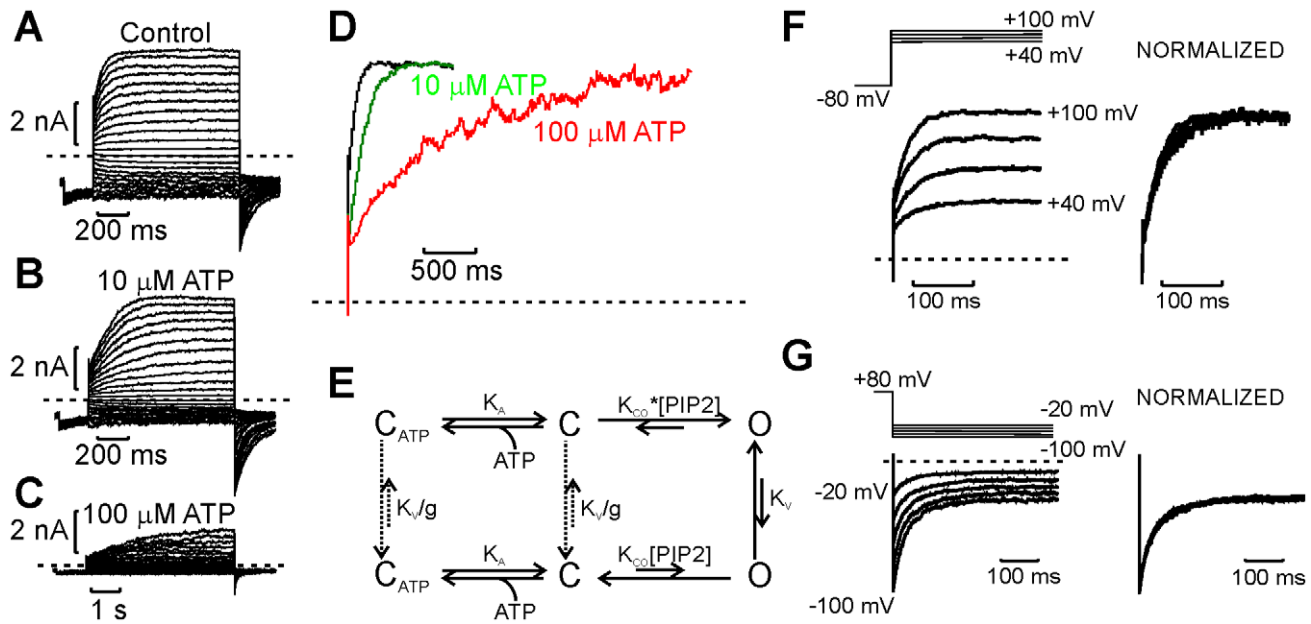


Figure 7. Predictions of gating coupled to changes in permeant ion occupancy. (A–C) In the presence of internal ATP, which acts by prolonging interburst intervals, the kinetics of channel activation are markedly slowed. (D) Normalized current traces recorded at +100 mV, in control and various internal ATP concentrations. (E) Extension of the scheme in Figure 3B, including ATP binding to closed states. In this scheme, ATP stabilizes the channel closed state, thereby prolonging the interburst intervals. (F,G) Kinetics of activation (F) and deactivation (G) and normalized in right-hand panels to illustrate very weak voltage dependence of kinetics.
doi:10.1371/journal.pbio.1000315.g007

and 50 mM K_{int} + 250 mM Na_{int} solutions, all buffer components were kept at the same concentration, with changes only to the indicated principal solutes (KCl or NaCl). Chemicals were all purchased from Sigma-Aldrich, or FLUKA, with the exception of PIP₂ (phosphatidylinositol 4,5-bisphosphate, Avanti).

Kinetic Modeling

Models describing steady-state voltage dependence of activation, and ion occupancy, were generated using the “Q-matrix

method” [58]. Matrix Q was constructed such that each element (i,j) was equal to the rate constant from state i to state j , and each element (i,i) was set to be equal to the negative sum of all other elements in row i . State occupancy at time t was calculated as $p(t) = p(0)e^{Qt}$, where $p(t)$ is a row vector containing elements corresponding to occupancy of each state in the model at time t . All tasks required for solving these equations were performed in MathCad 2000. Parameters describing ion occupancy are replicated from an earlier published model describing ion

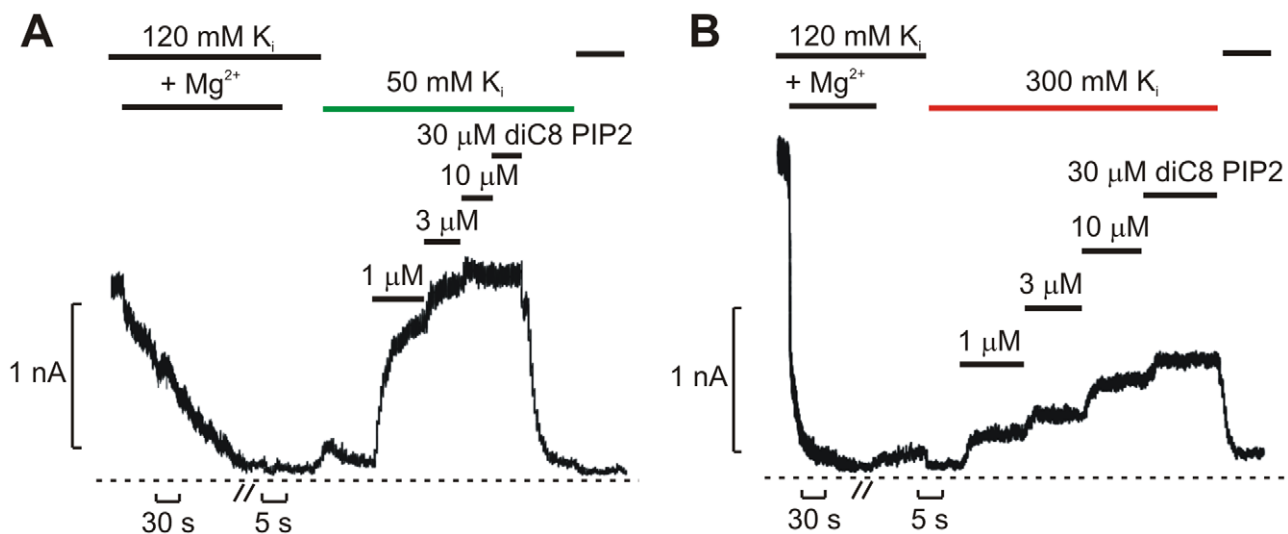


Figure 8. Ionic strength affects channel interactions with PIP₂. WT Kir6.2 channels were fully run-down in high Mg^{2+} and subjected to increasing concentrations of di-C8 PIP₂ in either (A) 50 mM or (B) 300 mM internal K^+ . PIP₂ results in more significant current recovery in low ionic strength conditions. Similar observations were made in six membrane patches.
doi:10.1371/journal.pbio.1000315.g008

permeation through KcsA channels, with the exception of a repulsion factor describing the interaction of ions in adjacent binding sites [40]. We reduced the published repulsion factor for the simulations described in Figure 6C, as we found this predicted higher cavity occupancy at extreme negative voltages.

Supporting Information

Figure S1 Voltage-dependent activation of L157E is position specific. (A) Pore-lining positions substituted with glutamate are highlighted in a molecular model of the Kir6.2 inner cavity. Position 157 is highlighted in red. (B–F) Currents elicited from inside-out membrane patches expressing each glutamate mutant. Pronounced voltage-dependent activation is only observed in Kir6.2[L157E] channels.

Found at: doi:10.1371/journal.pbio.1000315.s001 (0.16 MB TIF)

Figure S2 Polyamine block of Kir6.2[L157E] channels. Representative records depict voltage-dependent activation of Kir6.2[L157E] channels immediately after inside-out patch excision (A). In (B), voltage-dependent activation is abolished after saturation of open probability by application of PIP₂. (C) Complete and steeply voltage-dependent inhibition of outward currents in 100 mM spermine indicates that currents are carried through Kir6.2[L157E] and that effects of PIP₂ are not due to a non-specific leak or activation of another channel subtype.

Found at: doi:10.1371/journal.pbio.1000315.s002 (0.01 MB TIF)

Figure S3 Potassium and voltage-dependent effects on unitary currents in Kir6.2[L157E] channels and WT Kir6.2 channels. (A,B,C) Single channel records at –90 mV (left) and +90 mV, in various K_i conditions, as indicated. The properties of single channel currents vary dramatically between positive and negative voltages. At positive voltages, extremely long uninterrupted openings are apparent, whereas more frequent flicker-like closures are observed at negative voltages. Additionally, intracellular K⁺ dramatically affects open probability, with high K_i reducing channel P_o. (D) Similar features are also observed in WT Kir6.2 channels, with long openings observed at depolarized voltages and far more frequent flickering closures at negative

voltages. These marked asymmetries in the characteristics of single channel openings carrying inward versus outward currents may not be entirely surprising (given the asymmetric structure of an ion channel). These are included as somewhat anecdotal support for microscopic features of gating and permeation changing significantly with voltage. This asymmetry is especially apparent in low K_{int} conditions (Figure S3A), where negative voltages are characterized by rapid flicker-like closures, while no closures are observed at positive voltages.

Found at: doi:10.1371/journal.pbio.1000315.s003 (0.06 MB TIF)

Figure S4 Voltage-dependent activation of WT Kir6.2 channels. Inside-out patch-clamp recordings of WT Kir6.2 in symmetrical K⁺ concentrations, in the presence or absence of 10 μM ATP. We frequently observed modest activation of WT Kir6.2 at depolarized voltages (A). Though not as pronounced as in Kir6.2[L157E] channels, it is quite apparent and becomes more obvious in modest ATP concentrations (B). It is possible that experimental conditions can be devised to maximize this voltage dependence of WT Kir6.2.

Found at: doi:10.1371/journal.pbio.1000315.s004 (0.02 MB TIF)

Text S1 Where is the ligand/voltage-sensitive gate located? Supplemental text presents evidence related to the localization of the ATP/PIP₂-operated gate in Kir6.2 channels and ligand-operated gating in other Kir channels.

Found at: doi:10.1371/journal.pbio.1000315.s005 (0.06 MB DOC)

Acknowledgments

Many thanks to Peter Tunon, Tom Guiel, Brian Karger, Elizabeth Norseng, Shari Beharry, and Chad Ellis from Celectricon for their attention and assistance with the Dynaflo platform.

Author Contributions

The author(s) have made the following declarations about their contributions: Conceived and designed the experiments: HTK TB CGN. Performed the experiments: HTK MR MK. Analyzed the data: HTK. Contributed reagents/materials/analysis tools: HTK MR TB. Wrote the paper: HTK CGN.

References

- Long SB, Campbell EB, MacKinnon R (2005) Voltage sensor of Kvl.2: structural basis of electromechanical coupling. *Science* 309: 903–908.
- Ahern CA, Horn R (2005) Focused electric field across the voltage sensor of potassium channels. *Neuron* 48: 25–29.
- Bezanilla F (2008) How membrane proteins sense voltage. *Nat Rev Mol Cell Biol* 9: 323–332.
- Grabe M, Lai HC, Jain M, Jan YN, Jan LY (2007) Structure prediction for the down state of a potassium channel voltage sensor. *Nature* 445: 550–553.
- Tombola F, Pathak MM, Gorostiza P, Isacoff EY (2007) The twisted ion-permeation pathway of a resting voltage-sensing domain. *Nature* 445: 546–549.
- Tombola F, Pathak MM, Isacoff EY (2006) How does voltage open an ion channel? *Annu Rev Cell Dev Biol* 22: 23–52.
- Yellen G (2002) The voltage-gated potassium channels and their relatives. *Nature* 419: 35–42.
- Jiang Y, Ruta V, Chen J, Lee A, MacKinnon R (2003) The principle of gating charge movement in a voltage-dependent K⁺ channel. *Nature* 423: 42–48.
- Aggarwal SK, MacKinnon R (1996) Contribution of the S4 segment to gating charge in the Shaker K⁺ channel. *Neuron* 16: 1169–1177.
- Seoh SA, Sigg D, Papazian DM, Bezanilla F (1996) Voltage-sensing residues in the S2 and S4 segments of the Shaker K⁺ channel. *Neuron* 16: 1159–1167.
- Kubo Y, Baldwin TJ, Jan YN, Jan LY (1993) Primary structure and functional expression of a mouse inward rectifier potassium channel. *Nature* 362: 127–133.
- Kubo Y, Reuveny E, Slesinger PA, Jan YN, Jan LY (1993) Primary structure and functional expression of a rat G-protein-coupled muscarinic potassium channel. *Nature* 364: 802–806.
- Ho K, Nichols CG, Lederer WJ, Lytton J, Vassilev PM, et al. (1993) Cloning and expression of an inwardly rectifying ATP-regulated potassium channel. *Nature* 362: 31–38.
- Logothetis DE, Kurachi Y, Galper J, Neer EJ, Clapham DE (1987) The beta gamma subunits of GTP-binding proteins activate the muscarinic K⁺ channel in heart. *Nature* 325: 321–326.
- Nichols CG, Shyng SL, Nestorowicz A, Glaser B, Clement JP, et al. (1996) Adenosine diphosphate as an intracellular regulator of insulin secretion. *Science* 272: 1785–1787.
- Schulte U, Hahn H, Wiesinger H, Ruppersberg JP, Fakler B (1998) pH-dependent gating of ROMK (Kir1.1) channels involves conformational changes in both N and C termini. *J Biol Chem* 273: 34575–34579.
- Rohacs T, Chen J, Prestwich GD, Logothetis DE (1999) Distinct specificities of inwardly rectifying K(+) channels for phosphoinositides. *J Biol Chem* 274: 36065–36072.
- Matulef K, Zagotta WN (2003) Cyclic nucleotide-gated ion channels. *Annu Rev Cell Dev Biol* 19: 23–44.
- McCrossan ZA, Abbott GW (2004) The MinK-related peptides. *Neuropharmacology* 47: 787–821.
- Cordero-Morales JF, Cuello LG, Perozo E (2006) Voltage-dependent gating at the KcsA selectivity filter. *Nat Struct Mol Biol* 13: 319–322.
- Heginbotham L, LeMasurier M, Kolmakova-Partensky L, Miller C (1999) Single streptomyces lividans K(+) channels: functional asymmetries and sidedness of proton activation. *J Gen Physiol* 114: 551–560.
- Zagotta WN, Hoshi T, Aldrich RW (1994) Shaker potassium channel gating. III: Evaluation of kinetic models for activation. *J Gen Physiol* 103: 321–362.

23. Nilius B, Prenen J, Droogmans G, Voets T, Vennekens R, et al. (2003) Voltage dependence of the Ca^{2+} -activated cation channel TRPM4. *J Biol Chem* 278: 30813–30820.
24. Voets T, Droogmans G, Wissenbach U, Janssens A, Flockerzi V, et al. (2004) The principle of temperature-dependent gating in cold- and heat-sensitive TRP channels. *Nature* 430: 748–754.
25. Jara-Oseguera A, Llorente I, Rosenbaum T, Islas LD (2008) Properties of the inner pore region of TRPV1 channels revealed by block with quaternary ammoniums. *J Gen Physiol* 132: 547–562.
26. Sukhareva M, Hackos DH, Swartz KJ (2003) Constitutive activation of the Shaker Kv channel. *J Gen Physiol* 122: 541–556.
27. Inagaki N, Gonoi T, Clement JP, Namba N, Inazawa J, et al. (1995) Reconstitution of IKATP: an inward rectifier subunit plus the sulfonylurea receptor. *Science* 270: 1166–1170.
28. Clement JP, Kunjilwar K, Gonzalez G, Schwanstecher M, Panten U, et al. (1997) Association and stoichiometry of K(ATP) channel subunits. *Neuron* 18: 827–838.
29. Shyng S, Nichols CG (1997) Octameric stoichiometry of the KATP channel complex. *J Gen Physiol* 110: 655–664.
30. Shyng SL, Nichols CG (1998) Membrane phospholipid control of nucleotide sensitivity of KATP channels. *Science* 282: 1138–1141.
31. Baukrowitz T, Schulte U, Oliver D, Herlitze S, Krauter T, et al. (1998) PIP₂ and PIP as determinants for ATP inhibition of KATP channels. *Science* 282: 1141–1144.
32. Nichols CG (2006) KATP channels as molecular sensors of cellular metabolism. *Nature* 440: 470–476.
33. Kurata HT, Phillips LR, Rose T, Loussouarn G, Herlitze S, et al. (2004) Molecular basis of inward rectification: polyamine interaction sites located by combined channel and ligand mutagenesis. *J Gen Physiol* 124: 541–554.
34. Deutsch N, Matsuoka S, Weiss JN (1994) Surface charge and properties of cardiac ATP-sensitive K⁺ channels. *J Gen Physiol* 104: 773–800.
35. Loussouarn G, Pike IJ, Ashcroft FM, Makhina EN, Nichols CG (2001) Dynamic sensitivity of ATP-sensitive K(+) channels to ATP. *J Biol Chem* 276: 29098–29103.
36. Shyng S, Ferrigni T, Nichols CG (1997) Control of rectification and gating of cloned KATP channels by the Kir6.2 subunit. *J Gen Physiol* 110: 141–153.
37. Lorenz E, Alekseev AE, Krapivinsky GB, Carrasco AJ, Clapham DE, et al. (1998) Evidence for direct physical association between a K⁺ channel (Kir6.2) and an ATP-binding cassette protein (SUR1) which affects cellular distribution and kinetic behavior of an ATP-sensitive K⁺ channel. *Mol Cell Biol* 18: 1652–1659.
38. Phillips LR, Enkvetchakul D, Nichols CG (2003) Gating dependence of inner pore access in inward rectifier K(+) channels. *Neuron* 37: 953–962.
39. Phillips LR, Nichols CG (2003) Ligand-induced closure of inward rectifier Kir6.2 channels traps spermine in the pore. *J Gen Physiol* 122: 795–804.
40. Kutluay E, Roux B, Heginbotham L (2005) Rapid intracellular TEA block of the KcsA potassium channel. *Biophys J* 88: 1018–1029.
41. Jiang Y, Lee A, Chen J, Cadene M, Chait BT, et al. (2002) The open pore conformation of potassium channels. *Nature* 417: 523–526.
42. Berneche S, Roux B (2003) A microscopic view of ion conduction through the K⁺ channel. *Proc Natl Acad Sci U S A* 100: 8644–8648.
43. Enkvetchakul D, Nichols CG (2003) Gating mechanism of KATP channels: function fits form. *J Gen Physiol* 122: 471–480.
44. Enkvetchakul D, Loussouarn G, Makhina E, Nichols CG (2001) ATP interaction with the open state of the K(ATP) channel. *Biophys J* 80: 719–728.
45. Li L, Geng X, Drain P (2002) Open state destabilization by ATP occupancy is mechanism speeding burst exit underlying KATP channel inhibition by ATP. *J Gen Physiol* 119: 105–116.
46. Proks P, Ashcroft FM (2008) Modeling K(ATP) channel gating and its regulation. *Prog Biophys Mol Biol*.
47. Rohacs T, Lopes CM, Jin T, Ramdya PP, Molnar Z, et al. (2003) Specificity of activation by phosphoinositides determines lipid regulation of Kir channels. *Proc Natl Acad Sci U S A* 100: 745–750.
48. Armstrong CM (1971) Interaction of tetraethylammonium ion derivatives with the potassium channels of giant axons. *J Gen Physiol* 58: 413–437.
49. Del Camino D, Yellen G (2001) Tight steric closure at the intracellular activation gate of a voltage-gated K(+) channel. *Neuron* 32: 649–656.
50. Nishida M, Cadene M, Chait BT, MacKinnon R (2007) Crystal structure of a Kir3.1-prokaryotic Kir channel chimera. *EMBO J* 26: 4005–4015.
51. Kuo A, Gulbis JM, Antcliff JF, Rahman T, Lowe ED, et al. (2003) Crystal structure of the potassium channel KirBac1.1 in the closed state. *Science* 300: 1922–1926.
52. Heginbotham L, Kutluay E (2004) Revisiting voltage-dependent relief of block in ion channels: a mechanism independent of punchthrough. *Biophys J* 86: 3663–3670.
53. Rocheleau JM, Kobertz WR (2008) KCNE peptides differently affect voltage sensor equilibrium and equilibration rates in KCNQ1 K⁺ channels. *J Gen Physiol* 131: 59–68.
54. Horrigan FT, Aldrich RW (2002) Coupling between voltage sensor activation, Ca²⁺ binding and channel opening in large conductance (BK) potassium channels. *J Gen Physiol* 120: 267–305.
55. Martinez-Francois JR, Xu Y, Lu Z (2009) Mutations reveal voltage gating of CNGA1 channels in saturating cGMP. *J Gen Physiol* 134: 151–164.
56. Jogini V, Roux B (2005) Electrostatics of the intracellular vestibule of K⁺ channels. *J Mol Biol* 354: 272–288.
57. Flagg TP, Kurata HT, Masia R, Caputa G, Magnuson MA, et al. (2008) Differential structure of atrial and ventricular K-ATP atrial K-ATP channels require SUR1. *Circulation Research* 103: 1458–U228.
58. Colquhoun D, Hawkes AG (1995) A Q-matrix cookbook: how to write only one program to calculate the single-channel and macroscopic predictions for any kinetic mechanism. In: Sakmann B, Neher E, eds. *Single channel recording*. Plenum Press. pp 589–636.